

Automatic Classification of Aerial Imagery

Jharna Majumdar, Lekshmi S., and B. Vanathy

Aeronautical Development Establishment, Bangalore-560 093

ABSTRACT

The aerial imagery obtained from reconnaissance platform is voluminous and the defence forces rely on image information to perform intelligent tasks. The application of a well designed automatic image classifier would enhance the end results of different high level applications thereby abridging the effort of a human analyst. Automatic image classifiers could be designed using a training data set for supervised learning or using an unsupervised learning. In this paper, a method, which combines both unsupervised and supervised methods of learning is proposed.

Keywords: Aerial imagery, automatic image classifier, image information, surveillance, image processing algorithms, image classification

1. INTRODUCTION

The aerial imagery obtained from reconnaissance platforms is an important visual cue for extracting intelligent information. The images are voluminous and the defence forces rely on image information for various applications related to surveillance and reconnaissance, generation of knowledge-base of known/unknown areas, situation awareness, plan for future missions, etc.

Most of the tasks related to the development of an intelligent image processing system from imagery consist of subjecting the image to low-level, mid-level, and high-level image processing routines. The complexity in the development of image processing algorithms can range from the decision of a threshold value to the formulation of expert rules for multivariate data. The acquisition of aerial imagery in an unstructured and uncontrolled environment which adds to the complexity of the problem due to the dynamic change in the quality

of the incoming imagery. Depending on the change in the quality of the imagery, the appropriate image processing routine has to be applied automatically without any human intervention.

An interesting example could be the development of adaptive image enhancement routines for incoming video imagery during an aircraft flight mission. The repository contains all enhancement routines but to perform the decisive action of choosing the appropriate routine relies on the quality of the image, which is decided by the class of the image. A good classification of the incoming imagery would facilitate a better performance to adaptive enhancement. There are similar applications where image classification plays an important role and hence this particular research area is explored in this paper. Similar research has been carried out by Lukas and Walczak in the development of customised associative classifiers and by Lee and Warner for region-based classification approach¹⁻².

This paper describes the proposed approach to image classification, where a learning module is used to learn image class and an identification module to identify the class. Figure 1 shows the schematic sketch of the approach of classification.

2. CLASSIFICATION METHODOLOGY

The objective of this study is to classify the images from a large repository based on their properties. Although there exists a number of descriptors to represent an image, it is observed that properties from multiple attribute images derived from the input intensity image give better representation of the image. Two different approaches are used for feature definition to establish the convergence of the two methods towards a common classification scheme. The feature vectors are derived from the intensity, contrast, Weibull, and fractal images resulting in a 32-D vector. In addition, feature vectors from the texture images are also used which results in an 80-D vector. The feature vectors derived from the image using two entirely different approaches would help to independently analyse the robustness of the classification method.

To start with, each feature vector is subjected to dimensionality reduction and later to an unsupervised classification scheme to form the initial clusters representing images belonging to different classes. The cluster information is post-processed to find the class corresponding to each cluster. It could be observed that both statistical and texture feature vectors form almost similar clusters with the initial set of test images.

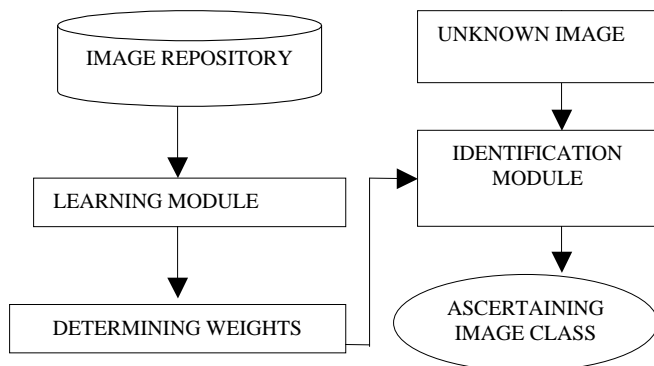


Figure 1. Schematic sketch of image classification.

In the next stage, the classification of the images is done using the results of cluster centres generated using statistical analysis. This is followed by supervised classification method using discriminant functions to assign weight to each feature. The weights are stored as references and are used for the classification of an unknown image.

The two stages of classification process are: (i) learning module and (ii) identification module. The block diagram of the classification algorithm is shown in Fig. 2(a). Figure 2(b) shows the verification module.

Verification module is to ascertain the correctness of the proposed classification approach. For this purpose, an unknown test image, identified as Class 1 image by identification module, is added to the repository. Its class is determined through unsupervised classification using clustering method. In a major experiment conducted using 60 images, it was found that almost in all the cases, the two approaches gave identical results.

2.1 Feature Extraction

2.1.1 Statistical Properties

The depiction of an image in the intensity domain alone has proved to be insufficient for unique identification in recognition and classification applications. The range of properties extracted from different classes of intensity images overlap, which makes it difficult to define a bounded interval for each class.

Unlike the conventional approach of considering intensity image alone, the different attributes of the image are explored viz., contrast, Weibull, and fractal derived from the intensity image.

(a) *Contrast image*: The contrast image captures the variation in contrast over local neighbourhood which could serve as a discriminating property over images of different classes. The contrast image is obtained from the intensity image using the transformation function

$$T(i, j) = \sqrt{\sum_{j=0}^3 (g(i, j) - M)^2}$$

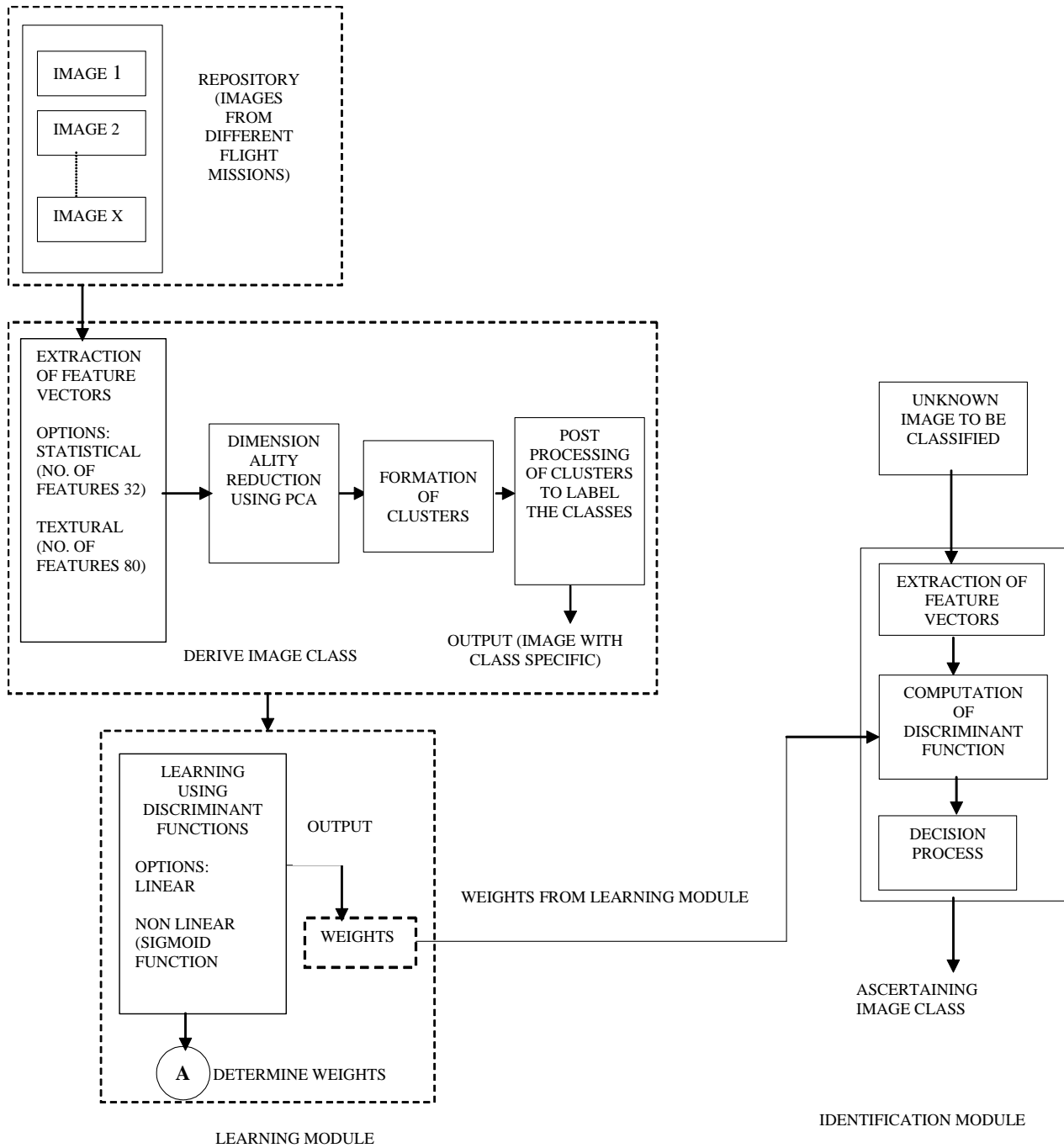


Figure 2. Block diagram of the classification method.

where $g(i, j)$ is the pixel of the image and M is the mean of the values.

(b) *Weibull image*: The Weibull image is generated using the form parameter of the Weibull distribution and captures the behaviour of data in spatial domain. It is obtained by mapping the scale

parameter of the Weibull distribution to the intensity range of the image.

The scale parameter of the Weibull distribution is $\beta_{m,n} = \exp\{\text{mean}[\ln(|C_{m,n}|)] + 0.5772/\gamma_{m,n}\}$, where $C_{m,n}$ is the pixel value and $\gamma_{m,n}$ given by $\gamma_{m,n} = \Pi / \text{std}[\ln(|C_{m,n}|)] \sqrt{6}$ is the form parameter³.

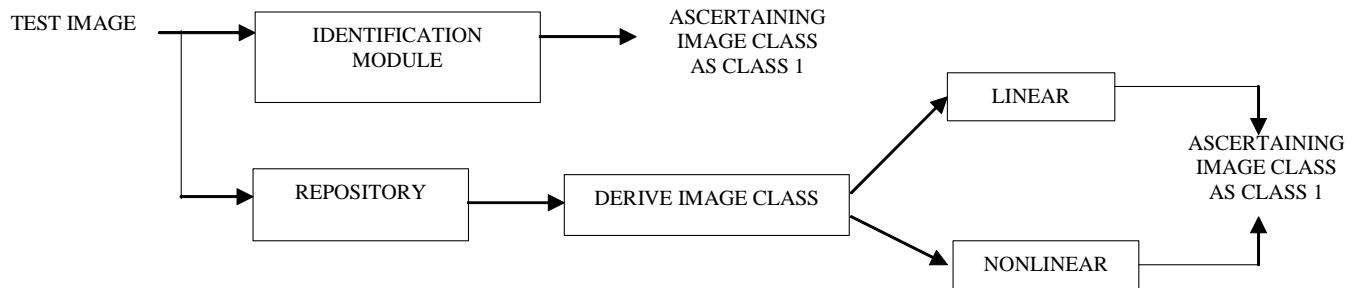
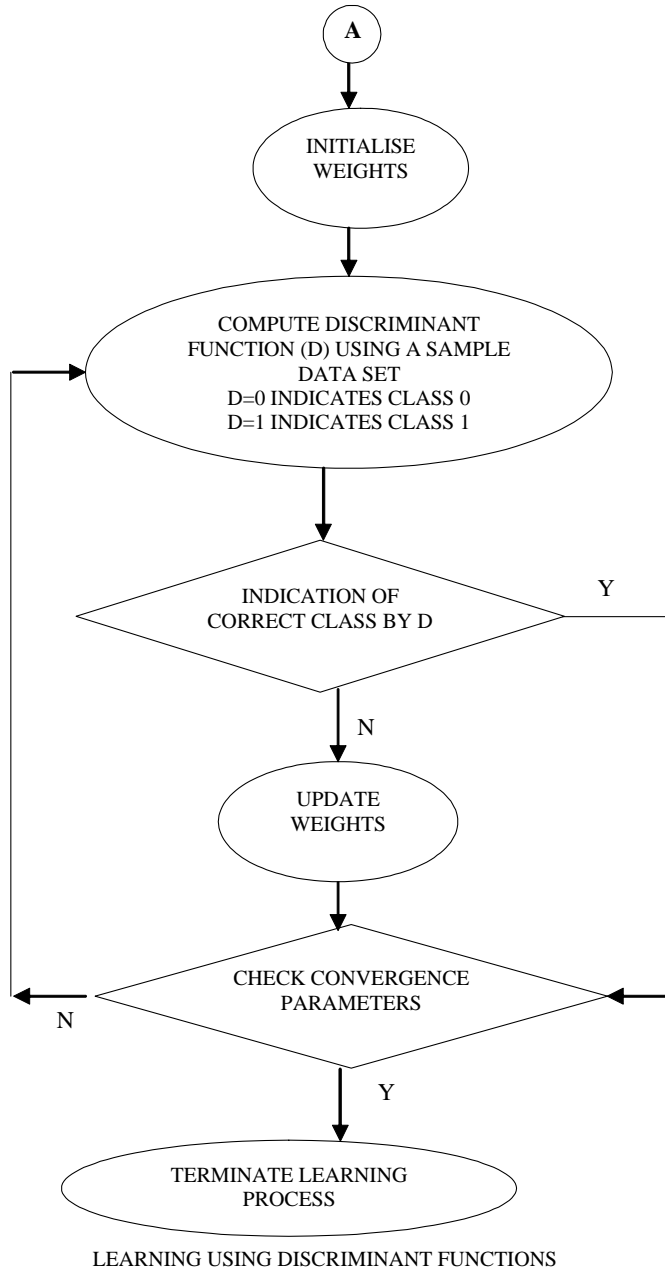


Figure 2(b). Block diagram of the verification module.

(c) *Fractal image*: The fractal image captures the structural information and is generated using the fractal dimension which is computed using variation method. The fractal image is obtained by mapping the fractal dimension computed locally to the intensity range of the image.

To compute the FD space, the difference V_ϵ between the maximum and the minimum gray-scale values is computed in a small window of size $T \times T$, where $T = 2\epsilon + 1$, centred at the pixel with coordinates (x,y) . This computation is repeated for all pixels (x,y) of the image, for $\epsilon = 1,2,3,\dots,\epsilon_{\max}$. $V_\epsilon(x,y)$ is the ϵ^{th} variation of the pixel located at (x,y) . E_ϵ is taken as the average of $V_\epsilon(x,y)$ over a window W of size $R \times R$. The slope of the line that best fits the points $(\log(R/\epsilon), \log \{(R/\epsilon)^3 E_\epsilon\})$ where $\epsilon = 1,2,3,\dots,\epsilon_{\max}$, and is the FD located at the window W and is assigned to the centre pixel⁴.

2.1.2 Texture Properties

This paper uses two different methods of texture analysis:

(a) *Grey level co-occurrence matrix*: The texture content of the image is captured using gray level co-occurrence matrix method which yields a set of six texture features for the image. The co-occurrence matrix defines the spatial relationship between any two pixels in an image as a function of distance and direction⁵. It gives the frequency of occurrence of a pair of intensity values in the given image. The six texture features extracted using cooccurrence method are:

- Angular second moment $\sum_{i,j=0}^{N-1} P_{i,j}^2$
- Entropy $\sum_{i,j=0}^{N-1} P_{i,j} (-\ln P_{i,j})$
- Contrast $\sum_{i,j=0}^{N-1} P_{i,j} (i-j)^2$

- Homogeneity $\sum_{i,j=0}^{N-1} \frac{P_{i,j}}{1+(i-j)^2}$
- Maximum probability $\text{Max} (P_{i,j})$
- Variance $\sigma_i^2 = \mu \sum_{i,j=0}^{N-1} P_{i,j} (i-j)^2$

Here, $P(i, j)$ denotes the probability of the co-occurrence of a pair of pixels.

(b) *Statistical geometric features*: Texture features can also be extracted based on the statistics of geometrical properties of connected regions in a sequence of binary images⁶. The first step of the approach is to decompose a texture image into a set of binary images. For each binary image, geometrical attributes such as the number of connected regions and their irregularity are statistically considered.

The first step of this method is to construct a stack of binary images. Consider a digital image $(n_x \times n_y)$ where n_x is the image length and n_y is the image width. Let the number of gray levels in the image be n_l . This image can be modelled by a two-dimensional function $f(x,y)$, where

$$(x, y) \in \{0,1,2,\dots,n_x - 1\} * \{0,1,2,\dots,n_y - 1\} \text{ and}$$

$$f(x, y) \in \{0,1,2,\dots,n_l - 1\}$$

This $f(x,y)$ is termed as the intensity of the image at (x,y) .

When an image $f(x,y)$ is thresholded with a threshold value α , $\alpha \in \{1,2,3,\dots,n_l-1\}$, a corresponding binary image is obtained, i.e.,

$$f_b(x,y; \alpha) = \begin{cases} 1 & \text{if } f(x,y) \geq \alpha \\ 0 & \text{otherwise} \end{cases}$$

where, $f_b(x,y; \alpha)$ denotes the binary image obtained with a threshold value α . From a given original image, there are n_l-1 different binary images, i.e., $f_b(x,y; 1), f_b(x,y; 2), f_b(x,y; 3), f_b(x,y; 4) \dots f_b(x,y; n_l-1)$. This set of binary images can be termed as binary stack.

The next step is to generate the geometrical attributes and its statistics from the binary images. For each binary image, all 1-valued pixels are grouped into a set of connected pixel groups termed as connected region and the same is done for 0-valued pixels. The number of connected regions of 1-valued pixels in the binary image $f_b(x,y; \alpha)$ denoted by $NOC_1(\alpha)$ and the number of connected regions of 0-valued pixels in the same binary image denoted by $NOC_0(\alpha)$ are computed. These $NOC_1(\alpha)$ and $NOC_0(\alpha)$ are functions of α , $\alpha \in \{1,2,3... n-1\}$

The two geometrical attributes $NOC_1(\alpha)$ and $NOC_0(\alpha)$ are characterised using the following formula:

$$\text{Sample mean} = \frac{1}{\sum_{\alpha=1}^{n-1} g(\alpha)} \sum_{\alpha=1}^{n-1} \alpha g(\alpha)$$

$$\text{Sample variance} = \frac{1}{\sum_{\alpha=1}^{n-1} g(\alpha)} \sum_{\alpha=1}^{n-1} (\alpha - \text{sample_mean})^2 \cdot g(\alpha)$$

where $g(\alpha)$ is one of the two functions $NOC_1(\alpha)$ and $NOC_0(\alpha)$.

3. EXTRACTION OF PROPERTIES FROM FEATURE IMAGES

The statistical and texture features derived from an image are further explored to define image properties. For this purpose, these features are normalised and mapped to the intensity domain as

shown in Fig. 3. From histogram of each of these feature images, a large number of properties are derived which would quantify the characteristics of the image.

The properties considered in this study are mean, standard deviation, entropy, skewness, kurtosis, separability, spatial frequency, and visibility

4. DIMENSIONALITY REDUCTION

Given a collection of features from the training images of all categories, the next question is how to reduce the dimensionality of feature space and select the most representative ones that would form a cluster. For this, principal component analysis (PCA) is used, where a multi-dimensional input data is viewed along its principal components or the eigen vectors of the data matrix^{10,11}. In this case the data matrix consists of the normalised values of the properties. The first three principal components are generally used for clustering since they give maximum discrimination as the eigen values drop immediately after the first three. The image properties are then projected back onto the axes corresponding to the principal components and taken as input for clustering. The computational complexity of the algorithm is $O[K(MN)^3]$, where K is the number of eigen values and M x N is the size of the image¹². In this study, the first three principal components are considered for clustering.

5. UNSUPERVISED LEARNING

The first three principal components obtained by dimensionality reduction are used for unsupervised

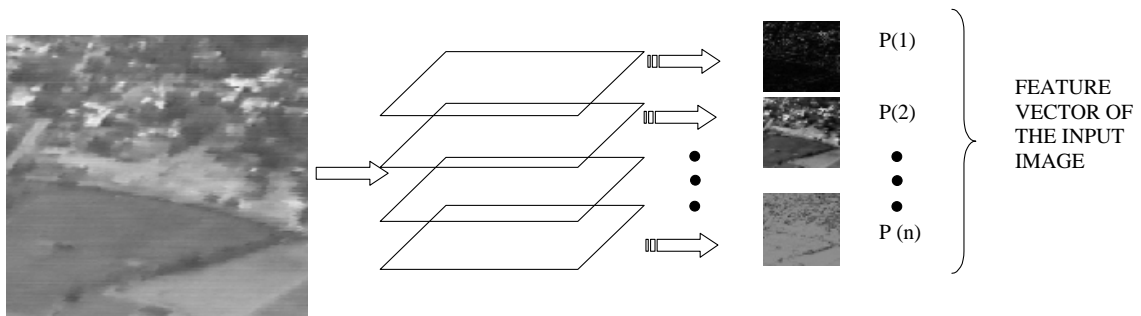


Figure 3. Input image and its representation in multiple attributes domain.

classification. Two clustering methods used in this study are the Batchelor Wilkins algorithm and the K Nearest-Neighbour algorithm. The Batchelor and Wilkins algorithm follows an iterative procedure to find newer cluster centres and the algorithm converges when the images that are associated with a cluster lie within the typical previous maximum distance. The K Nearest-Neighbours algorithm is another method used for clustering. It proceeds in levels from singletons to a final cluster, i.e., agglomerative method, or from one cluster down to many clusters, i.e., divisive method. The algorithm starts by selecting K Nearest-Neighbours to each point and then grouping the clusters based on their similarity and closeness. It could be observed that Batchelor and Wilkins algorithm performs better in the case of smaller dataset whereas the K Nearest-Neighbours algorithm performs better in case of larger dataset. The computational complexity of Batchelor and Wilkins algorithm is $O(n)$ and that of K means algorithm is $O(nk)$ ¹³.

6. POST-PROCESSING OF UNSUPERVISED RESULTS BY LIMITED LEARNING

The output of clustering identifies different groups of data exhibiting similar behaviour. This knowledge is not sufficient for any image interpretation tasks. Hence, post-processing of clustering results is performed to label the different clusters.

The properties and the RMS values of the properties of all the images in a particular class are computed. Then, for each individual property, the clusters are ranked from increasing to decreasing order based on the RMS values. As the image properties reflect the nature of the images, upon being sorted, the clusters get arranged in a proper order of increasing/decreasing image quality by comparing the progressive variation in property values. The sequence that occurs most frequently in the rank list is chosen by the number of hits a sequence gets. Here, there is no distinction between a sequence and the sequence in reverse order of arrangement. The sequence could be from good to bad quality or from bad to good quality.

The direction of the sequence in decreasing order of image quality is then determined using

one typical biasing property, which is the spatial frequency. Spatial frequency is observed to be a good discerning parameter for broad classification of best quality image and a poor quality image. The RMS values of the clusters on the extremes of the chosen sequence are compared for the particular property and a decision regarding the direction of the thread (sequence) is made. These ordered clusters are then assigned to respective classes. The learning set, so formed, will serve as input to the supervised classifier.

7. SUPERVISED LEARNING

The supervised classifiers are designed based on the learnt database obtained from the post-processed clustering outputs. The classifiers developed would accept the feature vector, which is of dimension 32 and outputs the category of the input image. The classifier is designed based on discriminant analysis.

In this approach, image classification is performed using discriminant analysis. Discriminant analysis defines discriminant functions (DF) which would decide the decision boundary for each class^{14,15}. In the present study, a multilevel tree structure is used for classification. In the first level, the input image is broadly classified into two classes and in the subsequent levels of the tree, the image is further divided into two more classes and the process is repeated. The structure for this representation is shown in Fig. 4. The two types of discriminant analyses performed in this study are linear and nonlinear discriminant functions.

7.1 Linear Discriminant Function

In the case of linear discriminant, the function is expressed as a linear combination of predictors. Each predictor is assigned weights and the output converges to 1 or -1 depending on the feature vector. A typical linear decision function (d) takes the form

$$d(x) = \sum_{i=1}^n w_0 + w_i x_i$$

The response of this function is based on a weighted sum of its inputs, where x_i represent the

feature vector corresponding to a pixel and w_i are the corresponding weights.

The weights are initialised before the iteration procedure starts and are updated during iterations, if the sum of product value, $d(x)$ does not lie within the error limit of the actual value (1 or -1). The iteration process for convergence is performed for a predefined number of iterations or a prespecified error tolerance in weight updation.

When $d(x) > 0$, the threshold element causes the output of the function to be +1, indicating that the feature vector x represents a particular class. The feature vector shall represent the other class when $d(x) < 0$. The decision boundary implemented by the function is obtained by setting the equation $d(x) = 0$ which is the equation of a hyper plane in n -dimensional space.

$$d(x) = \sum_{i=1}^n w_i x_i - w_0$$

$$w_0 + w_1 x_1 + w_2 x_2 + \dots + w_n x_n = 0$$

The complexity of the algorithm is $O(XYK^2)$ where K is the size of the feature set and $X \times Y$ is the size of the image.

7.2 Nonlinear Discriminant Functions

In the case of nonlinear discriminant, a sigmoid function is used to model the classification problem.

$$d(x) = \frac{e^{w_0 + \sum_{i=1}^n w_i x_i}}{1 + e^{w_0 + \sum_{i=1}^n w_i x_i}}$$

where f_i represent the feature vector corresponding to a pixel and w_i are the corresponding weights. The initialisation and updation of weights are performed as in the case of linear discrimination function. The output varies from 0 to 1 with convergence to 0 for one class and 1 for the other class. The complexity of the algorithm is $O[K(XY)^{5/2}M(XY)]$ where K is the size of the feature set and $X \times Y$ is the size of the image.

8. EXPERIMENTS AND RESULTS

In the present study, the classifiers using discriminant functions are designed for three class problems. The database for classification consists of a training database and a test database. The training database consists of 40 images, whereas the test database consists of 100 images of varying quality from different classes. Table 1 shows sample images

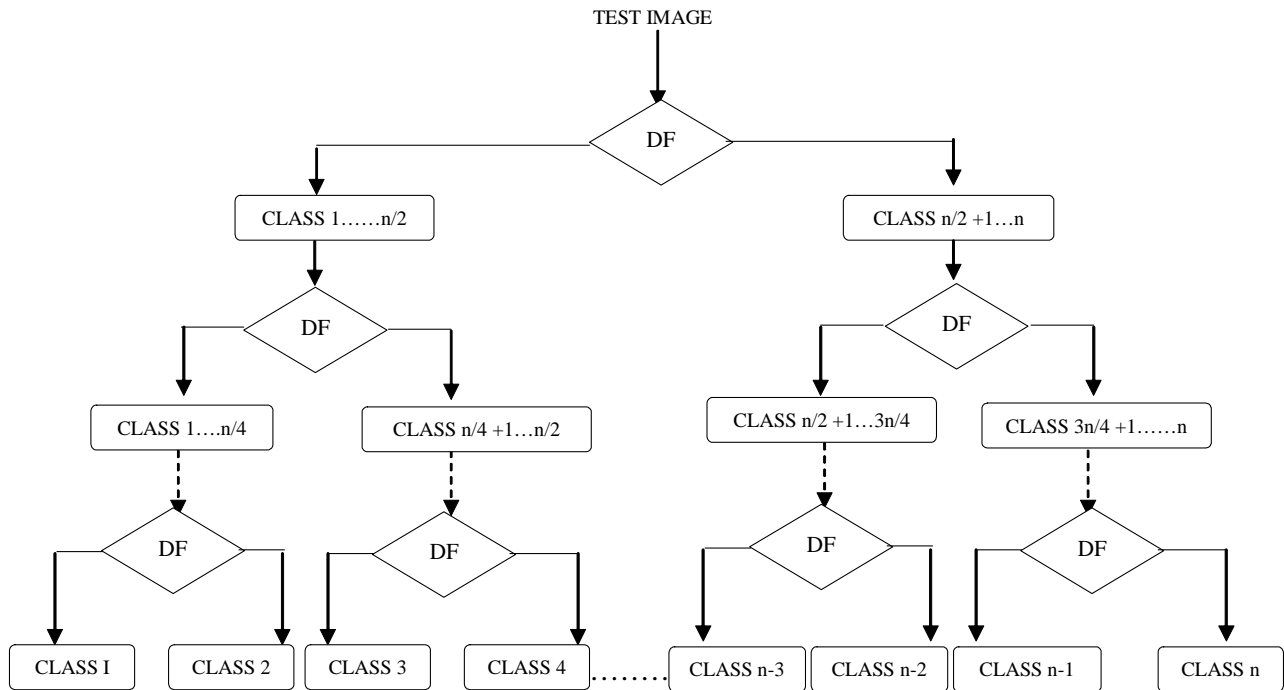


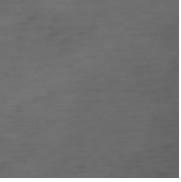
Figure 4. Representation of multi-level tree structure of discriminant analysis.

from each of the classes and the different statistical image properties in intensity, contrast, Weibull, and fractal domains.

After the extraction of properties, PCA is performed to reduce the dimension of the feature space. The

principal components are used to uniquely represent the data point in the reduced feature space. These feature points are used for clustering analysis and generate homogeneous groups. Figure 5 shows test images that form different classes and Figs 6(a) and (b) shows the output of clustering using Batchelor

Table 1. Properties of sample images of different classes: intensity domain (I), contrast domain (C), Weibull domain (W), and fractal domain (F)

IMAGES	 Class 1	 Class 2	 Class 3
1 Brightness (I)	142.16	145.87	111.53
2 Contrast (I)	55.39	32.38	3.78
3 Entropy (I)	7.68	6.91	3.76
4 Skewness (I)	0.38	0.68	0.68
5 Kurtosis (I)	-0.01	-0.60	0.01
6 Separability (I)	0.59	0.69	0.64
7 Spatial Frequency (I)	35.80	8.21	2.57
8 Visibility (I)	1005.49	598.61	104.89
9 Brightness (C)	40.47	14.71	4.26
10 Contrast (C)	32.76	14.39	5.75
11 Entropy (C)	6.71	5.09	2.74
12 Skewness (C)	1.16	2.03	5.36
13 Kurtosis (C)	2.11	37.63	945.01
14 Separability (C)	0.67	0.57	0.86
15 Spatial Frequency (C)	26.30	11.57	6.21
16 Visibility (C)	4499.35	8405.83	9822.34
17 Brightness (W)	142.39	156.98	149.80
18 Contrast (W)	52.77	58.94	43.85
19 Entropy (W)	7.53	7.69	7.29
20 Skewness (W)	0.59	0.77	0.94
21 Kurtosis (W)	0.42	-0.32	1.07
22 Separability (W)	0.56	0.69	0.62
23 Spatial Frequency (W)	27.19	20.32	20.63
24 Visibility (W)	931.39	957.84	736.33
25 Brightness (F)	153.76	113.03	81.78
26 Contrast (F)	24.78	26.00	16.79
27 Entropy (F)	5.68	5.33	4.58
28 Skewness (F)	1.93	1.29	0.55
29 Kurtosis (F)	20.97	5.04	17.08
30 Separability (F)	0.61	0.68	0.46
31 Spatial Frequency (F)	27.07	23.91	22.26
32 Visibility (F)	298.45	626.91	423.52

and Wilkins algorithm for both statistical and textural features. Tables 2(a) and 2(b) show the cluster output for the test data using statistical and texture features.

It could be observed that three images of Class 2 are getting misclassified to Class 3 in both the cases. A study of cluster distances shows that in the case of statistical features the distance between second and third clusters is less compared to the first and second clusters. Similarly, three images of Class 2 are getting misclassified to Class 1 for texture features since the distance between first and second cluster is less compared to that of second and third cluster. The study is carried forward using statistical features since the intra-cluster distance is higher in the case of clustering using statistical features.

The outputs are post-processed to find the sequence in which the clusters represent the images based on their quality. This information would serve as input for supervised learning. Figure 7 shows a test image for which the image class is to be determined.

Table 2(a). Clustering results using statistical features

Statistical	Class 1	Class 2	Class 3
Class 1	10 (0)	0 (154)	0 (158)
Class 2	0 (154)	17 (0)	3 (144)
Class 3	0 (158)	0 (144)	10 (0)

(Distance between the cluster centres is given in brackets)

Table 2(b). Clustering results using texture features

Texture	Class 1	Class 2	Class 3
Class 1	9 (0)	1 (149)	0 (125)
Class 2	3 (149)	17 (0)	0 (168)
Class 3	0 (125)	0 (168)	10 (0)

(Distance between the cluster centres is given in brackets)

The image shown in Fig. 7 belongs to Class 2. To classify the image using discriminant functions, image properties are extracted and are assigned appropriate weights, which are computed during the training phase of the classifier. To compute the

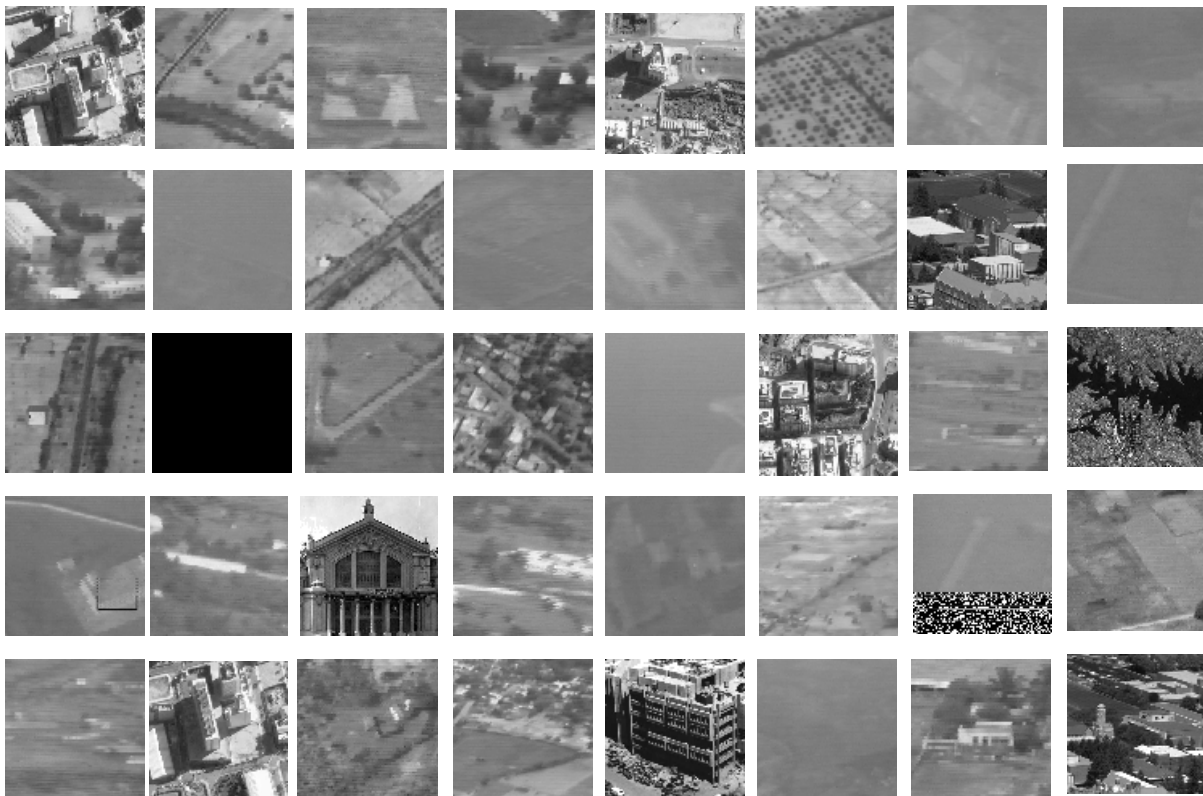


Figure 5. Training image data set.

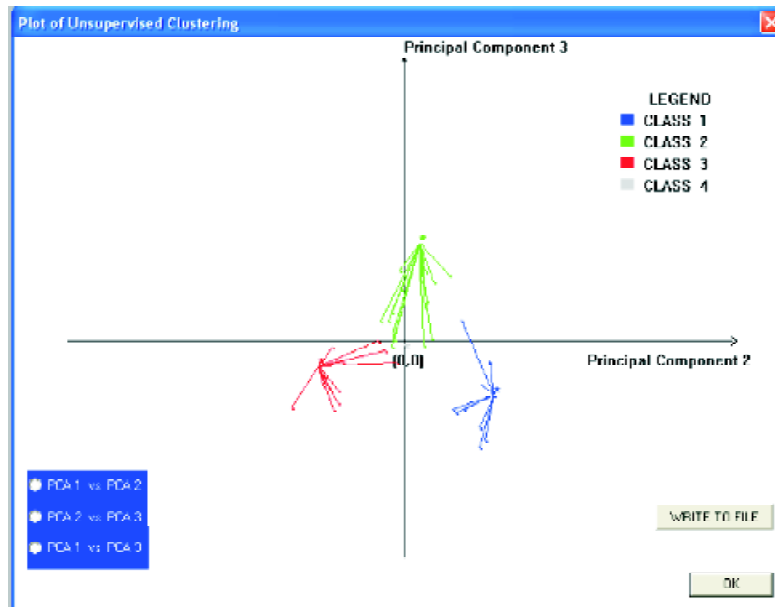


Figure 6(a). Clustering results using principal component analysis for statistical features.

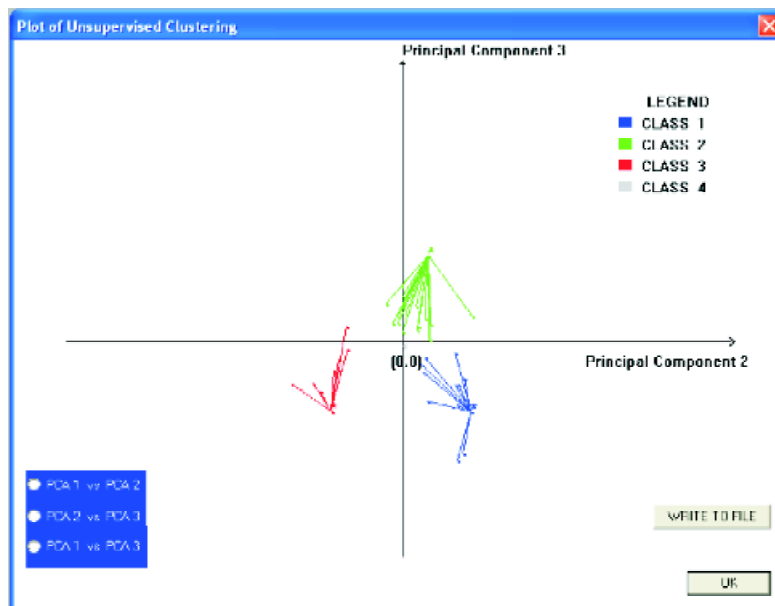


Figure 6(b). Clustering results using principal component analysis for texture features.

discriminant function, the weighted properties are summated or integrated, depending on the kind of classification. The images are classified using a binary tree structure.

In level 1, the initial classification broadly classifies the image set into two classes. In Level 2, it is further subdivided based on the image properties. Since a three class problem is being considered,

the tree will have an empty branch in the second level since all properties align towards the third class. The value of linear discriminant function in the first level is 4.53 which assigns the image to either first class or second class since $4.53 > 0$ (0 is the threshold). In the second level, it is assigned to second class since the value of discriminant function is -4.36 . The value of nonlinear discriminant function in the first level is 0.98 which assigns the



Property	Value	Property	Value	Property	Value
I (Mean)	0.59	C (Skewness)	0.29	W (Spatialfreq)	0.47
I (SD)	0.42	C (Kurtosis)	0.04	W (Visibility)	0.33
I (Entropy)	0.83	C (Separability)	0.14	F (Mean)	0.67
I (Skewness)	0.20	C (SpatialFreq)	0.20	F (SD)	0.76
I (Kurtosis)	0.07	C (Visibility)	0.58	F (Entropy)	0.79
I (Separability)	0.47	W (Mean)	0.82	F (Skewness)	0.38
I (SpatialFreq)	0.13	W (SD)	0.73	F (Kurtosis)	0.06
I (Visibility)	0.28	W (Entropy)	0.92	F (Separability)	0.52
C (Mean)	0.17	W (Skewness)	0.01	F (Spatialfreq)	0.44
C (SD)	0.23	W (Kurtosis)	0.09	F (Visibility)	0.09
C (Entropy)	0.51	W (Separability)	0.45		

Figure 7. Sample image of Class 2 and the normalised properties: intensity domain (I), contrast domain (C), weibull domain (W), and fractal domain (F).

image to either first class or second class since $0.98 > 0.5$ (0.5 is the threshold). In the second level, it is assigned to second class since the value of discriminant function is 0.03. The image is classified to Class 2 by both linear and nonlinear methods.

To verify the output, the image data are subjected to clustering with the unknown dataset. In the case of clustering, the image was grouped with the set of unknown images of the same category, which confirms the performance of the algorithm. The

Level 1			Level 2 - 1			Level 2 - 2		
Co-eff. Values for CLASS (1,2) & CLASS (3,4)			Co-eff. Values for CLASS (1) & CLASS (2)			Co-eff. Values for CLASS (3) & CLASS (4)		
Co-eff.	Linear	Non-Linear	Co-eff.	Linear	Non-Linear	Co-eff.	Linear	Non-Linear
a0	-1.000	-1.000	a0	-1.000	-1.000	a0	0.000	0.000
a1	0.282	0.482	a1	-2.944	-2.774	a1	-0.276	-0.276
a2	1.202	1.235	a2	0.522	0.673	a2	0.157	0.157
a3	1.223	1.120	a3	-0.388	-0.269	a3	0.249	0.249
a4	-2.575	-1.836	a4	-1.236	-1.769	a4	0.506	0.506
a5	-3.495	-2.886	a5	-0.385	-0.573	a5	0.310	0.310
a6	-0.185	-0.096	a6	-0.743	-0.729	a6	-0.291	-0.291
a7	1.306	0.916	a7	2.568	2.700	a7	0.217	0.217
a8	1.846	1.517	a8	2.684	2.755	a8	0.142	0.142
a9	1.009	0.544	a9	2.321	2.536	a9	0.290	0.290
a10	1.129	0.992	a10	1.913	2.064	a10	0.227	0.227
a11	0.471	0.343	a11	0.939	1.129	a11	0.358	0.358
a12	-1.218	-1.261	a12	-1.065	-1.228	a12	-0.363	-0.363
a13	-0.583	-0.646	a13	-0.120	-0.137	a13	-0.303	-0.303
a14	1.515	1.571	a14	0.192	0.378	a14	-0.055	-0.055
a15	0.807	0.603	a15	2.134	2.462	a15	0.221	0.221
a16	-0.652	-0.286	a16	-1.944	-2.055	a16	-0.487	-0.487
a17	0.563	0.148	a17	-0.548	-0.013	a17	-0.586	-0.586
a18	0.758	0.786	a18	-1.285	-1.414	a18	-0.446	-0.446
a19	1.628	1.661	a19	-1.825	-1.838	a19	-0.448	-0.448
a20	-2.569	-1.948	a20	-2.119	-2.833	a20	0.377	0.377
a21	-3.676	-3.184	a21	-0.639	-0.821	a21	0.330	0.330
a22	0.703	0.645	a22	-0.081	-0.095	a22	-0.321	-0.321
a23	1.642	1.268	a23	1.730	2.366	a23	-0.169	-0.169
a24	0.525	0.447	a24	-0.426	-0.943	a24	0.060	0.060
a25	1.607	1.534	a25	-0.360	-0.499	a25	0.510	0.510
a26	0.577	0.826	a26	-0.022	0.272	a26	0.595	0.595
a27	-0.694	-0.649	a27	-0.135	0.075	a27	0.727	0.727
a28	-0.944	-1.372	a28	-0.186	-0.494	a28	-0.544	-0.544
a29	-0.420	-0.555	a29	0.140	-0.223	a29	-0.712	-0.712
a30	-1.377	-1.367	a30	0.394	0.651	a30	-0.544	-0.544
a31	0.930	1.115	a31	0.786	0.908	a31	0.460	0.460
a32	-0.929	-0.889	a32	-0.133	-0.063	a32	-0.139	-0.139

Figure 8. Coefficients of discriminant functions for linear and nonlinear computation.

METHOD	CLASS 1	CLASS 2	CLASS 3
LINEAR	20	20	20
NONLINEAR	20	20	20

values of the coefficients of the discriminant functions for level 1 and level 2 are given in Fig. 8.

The supervised classifiers were tested for a database of 60 images, 20 from each class. All the images were correctly classified to their respective classes. Table 3 shows the results for linear and nonlinear classifiers.

9. CONCLUSIONS

The classification of UAV imagery using different classification methods is carried out in this study. The unsupervised approach of clustering methods is applied on the reduced feature set of the image database. The output of clustering method is post processed to label each cluster which would serve as the input to the supervised classifiers designed using linear and nonlinear discriminant analysis. The advantage of such an approach is that the user need not provide complete information about the application domain in the design phase of the classifier. The demerit of the approach is the choice of a large number of appropriate sample data to build the training database. Also, if additive noise is present in the image, it may tend to generate a wrong image class.

ACKNOWLEDGEMENT

The authors wish to express their heartfelt thanks to Mr G. Elangovan, Director, Aeronautical Development Establishment, Bangalore, for his constant encouragement and kind permission to publish this paper.

REFERENCES

1. www.konferencja2006.pti.katowice.pl/fimcsit/pliks/124.pdf.
2. www.isprs.org/istanbul2004/comm3/papers/438.pdf.
3. Fernandes, David. Segmentation of SAR images with Weibull distribution. *In International Geoscience and Remote Sensing Symposium (IGARSS)*, Seattle, 1998. pp. 1456-458.
4. Kasparis, T.; Charalampidis, D.; Georgiopoulos, M. & Rolland, J. Segmentation of textured images based on fractals and image filtering. *Pattern Recognition*, 2001, **34**, 1963-973.
5. Lohmann, G. Analysis and synthesis of textures: A co-occurrence-based approach. *CVGIP*, 1995, **19**(1), 29-36.
6. Chen, Y.Q.; Mark, S.N. & David, W. T. Statistical geometrical features for texture classification. *Pattern Recognition*, 1995, **28**(4), 537-52.
7. Chandra, B. & Majumdar, D. Dutta. Digital image processing and analysis. Prentice-Hall of India Pvt Ltd.
8. Gonzalez, Rafael C. & Richard Woods, E. Digital image processing, Ed. 2. Pearson Education Asia.
9. Jain, Anil K. Fundamentals of digital image processing. Prentice-Hall of India Pvt Ltd.
10. <http://beige.ucs.indiana.edu>.
11. <http://www.library.cornell.edu>.
12. Aykanat, Cevdet; Krpeoglu, brahim. & Dayar, Turul. *In 19th International Symposium on Computer and Information Sciences - ISCIS 2004*.
13. Daschiel, Herbert; Datcu, Mihai. Sebastino B. Serpico, *SPIE Proceedings*, 2003.
14. Bow, Sing-Tze. Pattern recognition and image processing. Marcel Dekker Inc.
15. Gose, Earl; Johnsonbaugh, Richard & Steve Jost. Pattern recognition and image analysis, PHI-2000.

Contributors



Ms Jharna Majumdar received her BTech (Hons) in Electronics and Electrical Engineering and Postgraduate Diploma in Computer Technology from Indian Institute of Technology, Kharagpur, in 1969 and 1970, respectively. She received her PhD in Electrical Engineering in 1980. She has about 34 years of research experience. She worked as Research Scientist in the area of robotics and automation at the Institute of Real Time Computer Systems and Robotics, Karlsruhe, Germany, during 1983 to 1989. Currently she is a Scientist and Head of Aerial Image Exploitation Division, Aeronautical Development Establishment (ADE), Bangalore. Her research areas include computer vision, artificial intelligence, and aerial image exploitation.



Ms Lekshmi S. graduated in Mathematics and postgraduated in Computer Science in 1995 and 1997, respectively. She received her PhD in Computer Science from University of Kerala in 2003. She worked as a Research Fellow for ISRO project and STEC project and was research associate of ADE (DRDO). Presently, she is working as a scientist in Aerial Image Exploitation Division, Aeronautical Development Establishment (DRDO), Bangalore. Her research areas are: Fractals, pattern recognition, astronomical image analysis and aerial image exploitation.



Ms B. Vanathy received her BE (Electronics and Comm Engg) and ME (Computer Science) in 1997 and 1999, respectively. Presently, she is working as a Scientist in Aerial Image Exploitation Division, ADE, Bangalore. Her research areas are: Registration, mosaicing, and aerial image exploitation.

This document was created with Win2PDF available at <http://www.daneprairie.com>.
The unregistered version of Win2PDF is for evaluation or non-commercial use only.